Image regularization for Poisson data

Journal of Physics: Conference Series **657** (2015) 012011 doi:10.1088/1742-6596/657/1/012011

Image regularization for Poisson data

A Benfenati[1] and V Ruggiero[2]

[1] [2] Polo Scientifico Tecnologico, Blocco B, Via G. Saragat, 1, 44120 Ferrara (FE)

E-mail: [1]alessandro.benfenati@unife.it, [2]valeria.ruggiero@unife.it

Abstract. Recently, Poisson noise has become of great interest in many imaging applications. When regularization strategies are used in the so-called Bayesian approach, a relevant issue is to find rules for selecting a proper value of the regularization parameter. In this work we compare three different approaches which deal with this topic. The first model aims to find the root of a *discrepancy* equation, while the second one estimates such parameter by adopting a *constrained* approach. These two models do not always provide reliable results in presence of low counts images. The third approach presented is the inexact Bregman procedure, which allows to use an overestimation of the regularization parameter and moreover enables to obtain very promising results in case of low counts images and High Dynamic Range astronomical images.

1. Introduction

In many imaging applications (e.g. astronomy, emission tomography) the detected image is affected by Poisson noise, due to the fluctuation of the incoming photons hitting the recording electronic device. All the pixels of the detected image $g \in \mathbb{R}^m$ can be considered as realizations of independent and identically distributed Poisson random variables G_i, $i = 1, \dots, m$; in a Bayesian approach [12], the unknown object $x \in \mathbb{R}^n$ is also considered as a realization of a multivalued random variable X and the *a priori* information is encoded into a given probability distribution (*prior*); an estimate of the source image can be obtained by maximizing the so–called posterior probability distribution of X or, equivalently, by solving the following minimization problem

$$\min_{x \geq 0} \varphi_\beta(Hx + b; g) \equiv \varphi_0(Hx + b; g) + \beta\varphi_1(x). \tag{1}$$

Here $\varphi_0(Hx + b; g)$ is the fit–to–data functional, which measures the discrepancy between the detected image g and the unknown image; φ_1 is the regularization function, which is assumed to be non–negative and convex, not necessarily differentiable; the problem is constrained since pixels' values are non–negative. $\beta \geq 0$ is a real parameter which measures the trade–off between φ_0 and φ_1 and it plays a role similar to that of the regularization parameter in Tikhonov theory. For an exhaustive treatment of the statistical model, see for example [5]. The imaging matrix $H \in \mathbb{R}^{m \times n}$ satisfies the assumptions $H_{i,j} \geq 0$, $\sum_{j=1}^{n} H_{i,j} > 0$; the non–negative term b is a constant background emission. Under the above assumptions, $\{x \geq 0 | Hx + b > 0\} \neq \emptyset$. Due to the presence of Poisson noise, a suitable choice for φ_0 is the generalized Kullback–Leibler divergence [5] $D_{\mathcal{KL}}(y; z) = \sum_{i=1}^{m} \left\{ y_i \log\left(\frac{y_i}{z_i}\right) + z_i - y_i \right\}$, with $y \log(y) = 0$ for $y = 0$. This function is non–negative, convex and coercive on its domain [11].

The quality of the restored image depends strongly on the β value used in (1). Unfortunately,

in presence of Poisson noise, such a value is very hard to estimate: in recent years several methods [2, 6] have been developed for this purpose. We mainly focus on the *Discrepancy Model* presented in [6, 18] and we will refer to it as **Model 1**. Several authors [9, 15], pointing out that such a model can require a considerably high computational effort, developed a *Constrained Model*: we will refer to it as **Model 2**. In [18] a comparison between the two models for some regularization functionals had been performed.
In presence of low counts images, we observe that both models do not always provide satisfactory results. A third approach, the Bregman procedure, which allows us to employ an *overestimation* of β, has been proposed for the Gaussian case [14]. Then, in [8], it was extended to the Poisson case; recently, in [3], in order to achieve a reasonable computational cost, an inexact procedure has been proposed. In this paper the inexact Bregman method is compared with Models 1 and 2 and it is shown that this scheme is very promising in terms of accuracy and efficiency for low counts images and for High Dynamic Range (HDR) images, when one is interested in detecting a weak signal close to very bright point sources.
The paper is organized as follows: in section 2 the basic ideas of the three models are recalled, in section 3 some numerical tests regarding the comparison between such models are presented together with an application concerning HDR images. Finally, the main conclusions are presented in section 4.

2. Descriptions of the models

In this section Model 1, Model 2 and the Bregman procedure are recalled; all the technical details can be found in the references listed in the text. We denote by x^* the true source image corresponding to the detected data g and by $x_\beta \geq 0$ the minimizer of (1) for a given β.

Model 1. In [17, 6] it is proved that when the expected value of each Poisson random variable $G_i,\ i = 1, \ldots, m$ is sufficiently large, the expected value for $D_{\mathcal{KL}}(g; Hx^* + b)$ is $m/2$. By defining the *discrepancy function* as $\mathcal{D}_H(x; g) = (2/m)D_{\mathcal{KL}}(g; Hx + b)$, the Discrepancy Model consists in finding a value for β such that

$$\mathcal{D}_H(x_\beta; g) = \eta \tag{2}$$

with η close to one. For several regularization functions, the minimizer of (1) exists and it is unique, and since $\mathcal{D}_H(x_\beta; g)$ is an increasing function of β, equation (2) admits one and only solution (see [6, 18]).

Model 2. The *Constrained Model* consists in solving the problem

$$\min_{x \geq 0} \varphi_1(x) \text{ subject to } \mathcal{D}_H(x; g) \leq \tau \tag{3}$$

for a given $\tau > 0$. In this case, only one minimization is required. Model 2 was firstly proposed in [15]. This formulation is linked with the estimation of β since one can write (3) as $\min_{x \geq 0} \varphi_1(x) + \lambda \left(\mathcal{D}_H(x; g) - \tau\right)$, where, following [6, 17], $\tau = \eta$: for a convenient value of λ (i.e. $\lambda = m(2\beta)^{-1}$), (3) and (2) have the same solutions. Indeed, in [18] under suitable assumptions on φ_1, it is proved that the two models provide the same parameter estimation, even in presence of non–negative data g, a very common situation in practical cases such as microscopy and astronomy.

Inexact Bregman Procedure. The main idea of the Bregman procedure [14, 8] consists in substituting φ_1 with its Bregman distance; the proposed inexact scheme [3] uses, in case of non differentiable regularization term, the ε–subgradients in computing such a distance, introducing the *inexact* Bregman distance. If φ is a convex function, its inexact Bregman distance from x to y is $\Delta_\varepsilon^\xi \varphi(x, y) = \varphi(x) - \varphi(y) - \langle \xi, x - y \rangle + \varepsilon$ with $\xi \in \partial_\varepsilon \varphi(y)$, $\varepsilon \geq 0$, where $\partial_\varepsilon \varphi(y)$ is the ε–subdifferential of φ at the point y. For differentiable regularization

term, $\varepsilon = 0$ and the subdifferential is the differential. The inexact Bregman scheme is an iterative procedure which at each step determines the approximate solution of the function $\psi_\beta(x; x^k) \equiv \varphi_0(Hx + b; g) + \beta\Delta^{\xi_k}_{\varepsilon_k}\varphi_1(x, x^k)$, where $\xi^k \in \partial_{\varepsilon_k}\varphi_1(x^k)$. The key idea of the procedure is to solve inexactly the minimization problem $\min \psi_\beta(x; x^k)$, stopping the inner iterative method when $\|\eta_{k+1}\|_2 \leq \mu_{k+1}$ and $\varepsilon_{k+1} \leq \nu_{k+1}$, with $\eta_{k+1} \in \partial_{\varepsilon_{k+1}}\psi_\beta(x; x^k)$, μ_k and ν_k such that $\sum_{i=1}^{\infty} \mu_i < \infty$, $\sum_{i=1}^{\infty} i\nu_i < \infty$. Under suitable assumptions [3, Proposition 4], the scheme converges to a minimizer of φ_0. For inverse problems, such as image restoration, the Bregman procedure (exact and inexact version) has the typical semiconvergence behaviour of the iterative methods. Thus, this procedure, coupled with an early stopping criterion, can be used as a regularization technique, without requiring an exact estimation of β. Indeed, a wide experimentation on low and high counts image confirms that an overestimation of β provides reliable results, with an enhancement of the contrast in the restored images and at the same time with a reasonable computational cost, in view of the inexact version of the procedure. This approach seems particularly efficient also in case of HDR images [4], when the Model 1 and the Model 2 do not always provide satisfactory results.

3. Numerical Experiments

In the following we describe a set of test-problems. For each problem, the optimal value β_{opt} is determined by trials, solving (1) for values of β uniformly distributed in an interval $[\beta_{\min}, \beta_{\max}]$; we define β_{opt} as the value corresponding to the minimum relative reconstruction error.

- **spacecraft**: the original image is a 256×256 image with sharp details, with values lying in $[0, 255]$ and the background b is 1; the imaging matrix is taken from `www.mathcs.emory.edu/~nagy/RestoreTools`. The ℓ_2 relative error from the detected data and the original image is 0.709139, β_{opt} is equal to $1.63 \cdot 10^{-3}$.
- **cameraman**: a 256×256 image with values in $[0, 3000]$. The imaging matrix derives from a Gaussian PSF with $\sigma = 1.3$; b is 0 and the ℓ_2 relative distance of g from x^* is 0.116422; β_{opt} is equal to $6.716 \cdot 10^{-3}$.
- **micro**: a confocal microscopy phantom of size 128×128 described in [16], with values in $[0, 69]$; the H matrix is the same used in [16]; b is 0. The relative ℓ_2 relative distance between the x^* and g is 0.190869; β_{opt} is $4.77 \cdot 10^{-2}$.

For all the three models, $\varphi_0 \equiv D_{\mathcal{KL}}$ and φ_1 is the Hyper Surface (**HS**) potential: $\varphi_1(x) = \sqrt{\sum_i \|\nabla_i x\| + \delta^2}$, where ∇_i is the discrete gradient at the i–th pixel and $\delta > 0$ (see [17] and references therein).
Model 1 and inexact Bregman method use as inner solver the Scaled Gradient Projection method [7]. Model 2 is implemented by an Alternating Directions Method of Multipliers, as specified in [15]. An adaptive rule for the selection of the parameter of this method is used (see [18]). In Table 1 the numerical results are reported. For cameraman, an high counts image, the three methods are equivalent, while for micro and spacecraft (low counts images) Model 1 and Model 2 do not achieve good results. Figure 1 shows the obtained restored images.

A common problem rising in astronomical imaging is the restoration of HDR images, i.e. images composed by very bright point sources of known position and faint diffuse objects around such sources. A suitable approach is to consider the signal as the sum of two terms [10], namely the point component x_p and the diffuse component x_d: $x = x_p + x_d$. Then, the restored image is obtained by regularizing the diffuse component only (see [4, 13] for details)

$$\min_{x \geq 0} D_{\mathcal{KL}}(g; Hx + b) + \beta\varphi_1(x_d). \tag{4}$$

The problems to which this strategy is applied are listed below. The evaluation of the models is done by computing the relative reconstruction error only on a window of interest of the diffuse component, located around the sources: this error is denoted by ρ_w.

Table 1. Comparison of the three models. In column–wise order: test problem, model, number of external iterations, total number of inner iterations, estimation of β, relative reconstruction error and time in secs. In the Bregman case, $\beta = 10\beta_{\text{opt}}$. The asterisk denotes that the maximum number of iterations allowed is reached.

Test problem	Model	k_{ext}	k_{tot}	β_k	err	time(s.)
cameraman	Model 1	8	815	$6.689 \cdot 10^{-3}$	$8.562 \cdot 10^{-2}$	16.67
	Model 2	451	–	$6.699 \cdot 10^{-3}$	$8.535 \cdot 10^{-2}$	30.28
	Bregman	6	3906	–	$8.730 \cdot 10^{-2}$	109.14
micro	Model 1	11	1458	$3.374 \cdot 10^{-3}$	$1.658 \cdot 10^{-1}$	9.77
	Model 2	*5000	–	$7.637 \cdot 10^{-3}$	$1.294 \cdot 10^{-1}$	94.41
	Bregman	9	4615	–	$8.370 \cdot 10^{-2}$	45.81
spacecraft	Model 1	41	3731	$1.000 \cdot 10^{-41}$	$1.000 \cdot 10^{0}$	258.73
	Model 2	*5000	–	$1.501 \cdot 10^{-4}$	$5.098 \cdot 10^{-1}$	360.20
	Bregman	9	27480	–	$3.780 \cdot 10^{-2}$	972.14

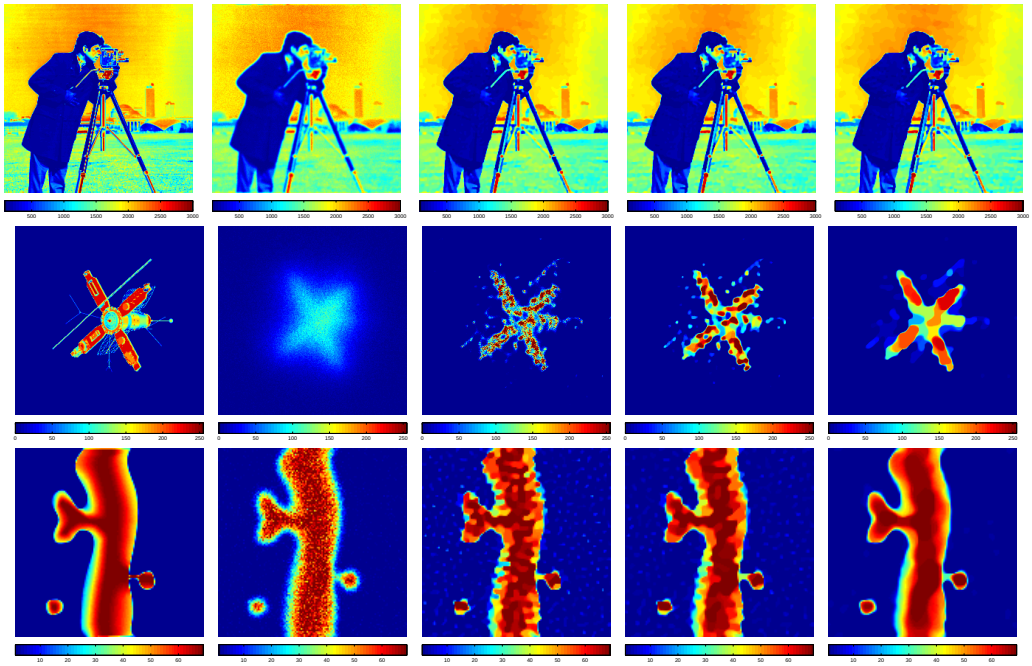

Figure 1. Visual inspection of the comparison. In column–wise order: original signal, blurred noisy images g, restored images by Model 1, Model 2 and inexact Bregman procedure, respectively.

- **YSO**: a 256×256 image of a single point source surrounded by a jet of circumstellar material. The imaging matrix is generated by means of `Software Package CAOS` [1], the relative ℓ_2 distance of g from x^* is 21.0254, b is $3.73 \cdot 10^3$. The source's intensity is $1.0184 \cdot 10^9$, while the maximum intensity on the x_d component is $2.3318 \cdot 10^6$ (see [4, 13]).
- **Binary Stars**: a 1024×1024 image with two point sources situated in a black disk at the centre of the diffuse component. H simulates the imaging matrix of a telescope. The ℓ_2 relative distance of g from x^* is 0.9823, b is 101.4. The point sources' intensities are $3.1411 \cdot 10^6$ while in the diffuse component the maximum value is $1.5200 \cdot 10^3$.

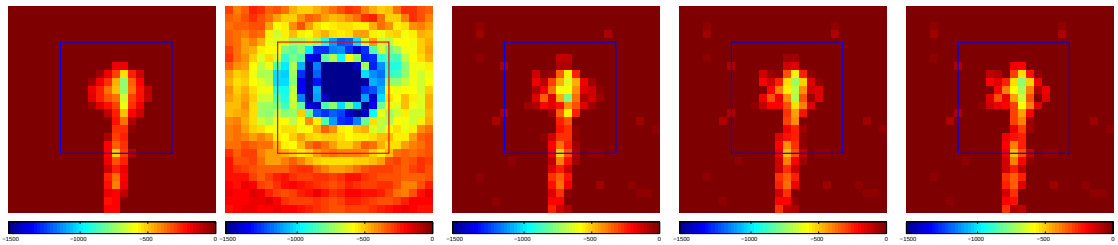

Figure 2. YSO reconstructions (particular). From left to right: x^*, g, Bregman procedure with Tikhonov regularization with $L = I$, $L = \nabla$ and $L = \nabla^2$ respectively. The highlighted square refers to the window on which ρ_w is computed. The images are displayed in a reverse square root scale.

For YSO problem, the Tikhonov regularization is used: $\varphi_1(x) = 1/2\|Lx\|_2$, with $L = I$ (identity matrix), $L = \nabla$ (discrete gradient) or $L = \nabla^2$ (discrete Laplacian). The optimal value for β is $1.6 \cdot 10^{-10}$, $5.0 \cdot 10^{-11}$ and $1.0 \cdot 10^{-11}$, respectively. In case of the Binary Stars, the **HS** regularization is used, β_{opt} is $5 \cdot 10^{-6}$. The solver used is SGP.

Table 2. YSO numerical results. φ_1 is the regularization function, β_{est} is the computed estimate, k_{ext} the number of external iterations, k_{tot} the total number of inner iterations and ρ_w is the relative reconstruction error of the window of interest. In the Bregman case, the β value denotes the value used in the procedure.

	Model 1				Inexact Bregman			
φ_1	β_{est}	k_{ext}	k_{tot}	ρ_w	β	k_{ext}	k_{tot}	ρ_w
$L = I$	$3.0 \cdot 10^{-9}$	11	6286	0.69	$2.0 \cdot 10^{-9}$	20	3590	0.3292
$L = \nabla$	$1.4 \cdot 10^{-9}$	10	5828	0.23	$0.4 \cdot 10^{-9}$	16	5287	0.3368
$L = \nabla^2$	$5.3 \cdot 10^{-10}$	9	4064	0.47	$3.3 \cdot 10^{-10}$	63	10071	0.2547

Table 2 shows the numerical results regarding the YSO problem. We observe that Model 1 can not achieve the optimal value for β, and does not provide reliable results. On the other hand, the inexact Bregman procedure allows to obtain satisfactory results even with a raw overestimation of the regularization parameter (Figure 2).

Finally, in Figure 3 the restoration of the image regarding the Binary Stars is presented. We

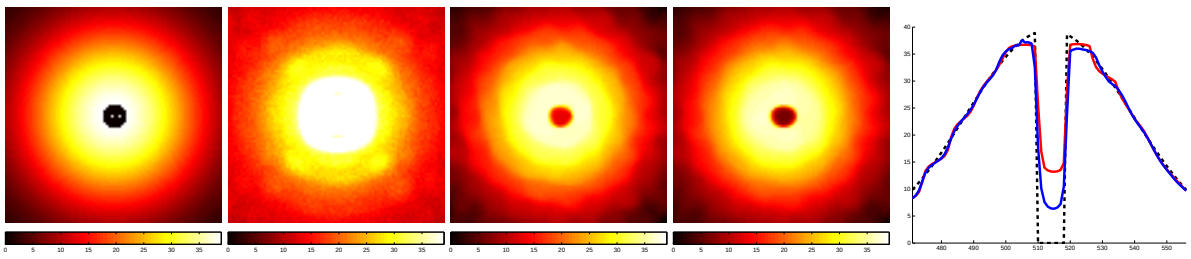

Figure 3. Binary star, window of interest. From left to right: x^*, g, restored image by SGP with β_{opt}, restored image at the 32th external iteration by Bregman procedure with $10\beta_{\text{opt}}$. The final panel is the superposition plot of the 513th line of x_d. The black dashed line is the original object, the red one refers to SGP reconstruction while the blue one refers to inexact Bregman reconstruction.

compare the results of Bregman procedure with the reconstruction obtained by solving (4) with

SGP method with $\beta = \beta_{\text{opt}}$. In such a way, the restored image shown in Figure 3 (3rd panel) is obtained in 178 iterations with a reconstruction relative error of 0.0941. Using the same method as inner solver in the inexact Bregman procedure, after 32 external iterations and 362 total inner iterations we obtain the reconstruction shown in Figure 3 (4th panel) where $\rho_w = 0.0822$: this result is achieved by setting $\beta = 10\beta_{\text{opt}}$. From the superposition plot of the line of diffuse data x_d related to the two stars (Figure 3, 5th panel), we can observe that the inexact Bregman procedure can reach the bottom of the central disk more precisely than the minimization of $D_{\mathcal{KL}} + \beta_{\text{opt}}\varphi_1$: this is due to the enhancing contrast feature of the inexact Bregman procedure.

4. Conclusions

In this work, the inexact Bregman procedure is compared with two different approaches for the estimate of the regularization parameter in presence of Poisson noise. It is shown that in case of high counts images the three models have a very similar behaviour, while for low counts images, and for HDR images, Model 1 and Model 2 do not provide satisfactory results. The Bregman procedure, instead, allows to treat such images and moreover permits to use an overestimation of the regularization parameter and at the same time to have a contrast enhancing.

References

[1] Arcidiacono C, Diolaiti E, Tordi M, Ragazzoni R, Farinato J, Vernet E and Marchetti E 2004 Layer-oriented simulation tool *Applied Optics IP* **43** 4288–4302
[2] Bardsley J M and Luttman A 2009 Total variation–penalized Poisson likelihood estimation for ill–posed problems *Adv. Comput. Math.* **31** 35–59
[3] Benfenati A and Ruggiero V 2013 Inexact Bregman iteration with an application to Poisson data reconstruction *Inverse Problems* **29**(6) 1–32
[4] Benfenati A and Ruggiero V 2015 Inexact Bregman iteration for deconvolution of superimposed extended and point sources *Communications in Nonlinear Science and Numerical Simulation* **20** 882–96
[5] Bertero M, Boccacci P, Desiderà G and Vicidomini G 2009 Image deblurring with Poisson data: from cells to galaxies *Inverse Problems* **25** 123006
[6] Bertero M, Boccacci P, Talenti G, Zanella R and Zanni L 2010 A discrepancy principle for Poisson data *Inverse Problems* **26** 10500
[7] Bonettini S, Zanella R and Zanni L 2009 A scaled gradient projection method for constrained image deblurring *Inverse Problems* **25** 015002
[8] Brune C, Sawatzky A and Burger M 2009 Bregman–TV–EM methods with application to optical nanoscopy, (Scale Space and Variationale Methods in Computer Vision) ed Tai X C et al Berlin : Springer 235–46
[9] Carlavan M and Blanc-Fèraud L 2012 Sparse Poisson noisy image deblurring *IEEE Trans. Image Process.* **21**(4) 1834-46
[10] De Mol C and Defrise M 2004 Inverse imaging with mixed penalties *Proceedings URSI EMTS 2004* (Ed. PLUS Univ. Pisa) 798–800
[11] Figueiredo M A T and Bioucas-Dias J M 2010 Restoration of Poissonian images using alternating direction optimization *IEEE Transactions on Image Processing* **19**(12) 3133–45
[12] Geman S and Geman D 1984 Stochastic relaxation, Gibbs distribution and the Bayesian restoration of images *IEEE Trans. Pattern Analysis and Machine Intelligence* **6** 721–41
[13] La Camera A, Antoniucci S, Bertero M, Boccacci P, Lorenzetti D, Nisini B and Arcidiacono C 2014 Reconstruction of high dynamic range images: simulations of LBT observations of a stellar jet, a pathfinder study for future AO–assisted giant telescopes *Publications Astron. Soc. Pacific* **126** 180–93
[14] Osher S, Burger M, Goldfarb D, Xu J and Yin W 2005 An iterative regularization method for total variation-based image restoration *SIAM Journal on Multiscale Modeling and Simulation* **4**(2) 460–89
[15] Teuber T Steidl G and Chan R H 2013 Minimization and parameter estimation for seminorm regularization models with I-divergence constraints *Inverse Problems* **29** 035007
[16] Willett R M and Nowak R D 2003 Platelets: A multiscale approach for recovering edges and surfaces in photon limited medical imaging *IEEE Transactions on Medical Imaging* **22** 332–50
[17] Zanella R, Boccacci P, Zanni L and Bertero M 2009 Efficient gradient projection methods for edge-preserving removal of Poisson noise *Inverse Problems* **25** 045010
[18] Zanni L, Benfenati A, Bertero M and Ruggiero V 2014 Numerical methods for parameter estimation in Poisson data inversion *Journal of Mathematical Imaging and Vision* Springer US